Published in final edited form as:
J Neurochem. 2009 October ; 111(2): 522–536. doi:10.1111/j.1471-4159.2009.06333.x.

Astrocytes are poised for lactate trafficking and release from activated brain and for supply of glucose to neurons

Gautam K. Gandhi[1], **Nancy F. Cruz**[2], **Kelly K. Ball**[2], and **Gerald A. Dienel**[1,2]

[1]Department of Physiology and Biophysics, University of Arkansas for Medical Sciences, Little Rock, Arkansas, 72205, USA

[2]Department of Neurology, University of Arkansas for Medical Sciences, Little Rock, Arkansas, 72205, USA

Abstract

Brain is a highly-oxidative organ, but during activation, glycolytic flux is preferentially upregulated even though oxygen supply is adequate. The biochemical and cellular basis of metabolic changes during brain activation and the fate of lactate produced within brain are important, unresolved issues central to understanding brain function, brain images, and spectroscopic data. Because in vivo brain imaging studies reveal rapid efflux of labeled glucose metabolites during activation, lactate trafficking among astrocytes and between astrocytes and neurons was examined after devising specific, real-time, sensitive enzymatic fluorescent assays to measure lactate and glucose levels in single cells in adult rat brain slices. Astrocytes have a 2-4-fold faster and higher capacity for lactate uptake from extracellular fluid and for lactate dispersal via the astrocytic syncytium compared to neuronal lactate uptake from extracellular fluid or shuttling of lactate to neurons from neighboring astrocytes. Astrocytes can also supply glucose to neurons as well as glucose can be taken up by neurons from extracellular fluid. Astrocytic networks can provide neuronal fuel and quickly remove lactate from activated glycolytic domains, and the lactate can be dispersed widely throughout the syncytium to endfeet along the vasculature for release to blood or other brain regions via perivascular fluid flow.

Keywords

astrocyte; neuron; connexin; gap junction; lactate; glucose

Glucose is the primary, obligatory fuel for brain, and glucose metabolism-based assays have, therefore, been a cornerstone of non-invasive imaging and spectroscopic studies of brain function and disease for decades. In the late 1960's, metabolic studies using labeled tracers were initiated to identify brain fuel, define compartmentation of utilization of minor substrates by neurons and astrocytes, assess astrocyte-neuron metabolic interactions, and calculate glucose utilization rates. Enormous progress has been made in understanding function-metabolism relationships but the cellular contributions to brain energy metabolism and brain images are not yet clear. Under resting conditions, nearly all of the glucose is oxidized and the metabolic ratio of oxygen to glucose utilization is close to the theoretical maximum of 6 (i.e.,

Corresponding Author: Gerald A. Dienel, Ph.D., University of Arkansas for Medical Sciences, Department of Neurology, Slot 830, Shorey Building, Room 715, 4301 West Markham Street, Little Rock, AR 72205, Phone (501) 603-1167, Fax (501) 296-1495, gadienel@uams.edu.

COMPETING FINANCIAL INTERESTS

The authors declare that they have no competing financial interests.

$6O_2$ + 1 glucose → $6CO_2$ + 6 H_20), but during brain activation this metabolic ratio generally, but not always, falls even though oxygen delivery is adequate (reviewed by Dienel and Cruz, 2004, 2008). The basis for the preferential rise in non-oxidative metabolism of glucose during activation is not understood, and increased lactate production that exceeds its oxidation is inferred.

The cellular origin and fate of lactate and the contribution of lactate to brain energetics in normal, activated brain are important, unresolved issues. In vivo experiments to define roles of endogenously-generated lactate are technically difficult, and the lack of consensus in the field is reflected by the diversity of current metabolic models. (i) Lactate generated by astrocytes during excitatory glutamatergic neurotransmission is hypothesized to be shuttled to neurons as a major fuel (Pellerin and Magistretti, 1994; Pellerin et al., 2007; Hyder et al., 2006), but glutamate-induced stimulation of glucose utilization and lactate production in cultured astrocytes is not a universal finding, the fate of pyruvate/lactate is not known, many laboratories find no glycolytic response to glutamate, and glutamate does stimulate astrocytic respiration (Chih and Roberts, 2003; Dienel and Cruz, 2004). (ii) Lactate is proposed to be the major oxidative substrate for brain mitochondria (Schurr, 2006), but this is quite unlikely because lactate dehydrogenase activity is commonly used as a marker for removal of cytoplasmic enzymes from ‘free’ (non-synaptosomal) mitochondria, and <1% of total lactate dehydrogenase activity is typically associated with purified mitochondria (e.g., Sims, 1990). (iii) Redox coupling mechanisms involving lactate-pyruvate exchange shuttles can link glycolytic and oxidative domains of heterogeneously-activated cells (Cerdán et al., 2006). (iv) Glucose is considered as the major fuel for activated brain cells and astrocyte-to-neuron lactate shuttling is questioned (Chih and Roberts, 2003; Korf, 2006; Hertz et al., 2007; Mangia et al., 2009a). (v) Increased glucose utilization during brain activation is linked to glycolytic upregulation, with rapid, substantial lactate release from activated tissue that predominates over any lactate shuttling plus local oxidation (Collins et al., 1987; Ackermann and Lear, 1989; Lear and Ackermann, 1989; Lear, 1990; Dienel and Cruz, 2004, 2008). (vi) Metabolic modeling predicts that predominant neuronal glucose utilization causes lactate transients in neurons with neuron-to-astrocyte lactate shuttling (Simpson et al., 2007; Mangia et al., 2009b). The available data from in vivo studies are not sufficient to identify the cellular origin of lactate produced during activation or the fate of that lactate, but in vivo metabolic studies in normal conscious subjects strongly support the predominance of lactate release from activated tissue.

The first line of evidence for upregulation of glycolysis and lactate release came from metabolic activation studies using two labeled glucose utilization tracers, one of which, glucose, generates diffusible labeled metabolites, whereas the other, 2-deoxyglucose, is metabolized to compounds that are retained intracellularly (Sokoloff et al., 1977). Underestimation of metabolic activation by [6-^{14}C]glucose, by 50% or more, arose from incomplete [^{14}C] metabolite retention and was ascribed to enhanced [^{14}C]lactate production and release from brain (Collins et al., 1987; Ackermann and Lear, 1989; Lear and Ackermann, 1989; Lear, 1990). [^{14}C]Glucose-derived lactate has a high specific activity, and, during spreading depression, rapid efflux of labeled and unlabeled lactate to cerebral venous blood accounted for half of the underestimation of [6-^{14}C]glucose utilization rate (Adachi et al., 1995; Cruz et al., 1999; Dienel and Cruz, 2009). During acoustic stimulation, tonotopic metabolic activation bands are strongly registered by [^{14}C]deoxyglucose compared to [1- and 6-^{14}C]glucose, and enhancement of [^{14}C]glucose band intensity by blockade of lactate transporters and gap junctions is consistent with increased spreading of ^{14}C from ^{14}C-labeled lactate and glutamine and elevated extracellular lactate levels during acoustic stimulation (Cruz et al., 2007). Together, these findings suggest that lactate clearance from activated cells in the inferior colliculus is mediated mainly by astrocytes, which are extensively gap junction-coupled forming syncytia comprised of thousands of cells (Ball et al., 2007). The goal of this study

was, therefore, to evaluate the capacity for lactate trafficking among astrocytes and from astrocytes to neurons in the inferior colliculus, the brain structure with the highest rates of blood flow and glucose utilization (Sokoloff et al., 1977; Gross et al., 1987). First, it was necessary to devise sensitive, specific, real-time methods to quantify metabolite levels in single cells, and enzymatic fluorescence assays were used to quantify uptake and shuttling of lactate and glucose among astrocytes and neurons in adult rat brain slices. The results demonstrate that (i) astrocytic lactate transport system is much faster and has higher capacity compared to that in neurons and (ii) astrocytes can supply glucose to nearby neurons.

MATERIALS AND METHODS

Brain slice preparation

Adult male Wistar-Hanover rats (300–350g, Taconic Farms, Germantown, NY)) were anesthetized with halothane, decapitated, and their brains were quickly removed and chilled by immersion in oxygenated (i.e., bubbled with O_2/CO_2, 95:5%), ice-cold artificial cerebral spinal fluid (aCSF) solution (concentrations in mmol/L: 26 $NaHCO_3$, 10 glucose, 124 NaCl, 2.8 KCl, 2.0 $MgSO_4$, 1.25 NaH_2PO_4, 2.0 $CaCl_2$, pH 7.3) and 248 mmol/L sucrose, and 250 μm-thick slices were prepared as described (Moyer and Brown, 1998). Coronal sections of midbrain (including inferior colliculus) were cut using a Leica (Heidelberg, Germany) VT 1000S tissue slicer, and inferior colliculus slices were incubated in oxygenated aCSF containing sucrose for 30 minutes at 35°C, then for 1 h at 22°C.

Microinjections

Slices of inferior colliculus were transferred to an open bath perfusion chamber (Warner Instruments, Hamden, CT) on the microscope stage and perfused (1 ml/min) with aCSF containing 10 mmol/L glucose, except for some glucose transfer assays that were carried out in the presence or absence of 10 μmol/L cytochalasin B (Sigma-Aldrich, St. Louis, MO) in the perfusion solution to inhibit glucose transport. In these experiments the perfusion medium was supplemented with pyruvate (10 mmol/L) as an oxidative fuel to compensate for glucose transport blockade. Perfusion solutions were freshly prepared, kept at room temperature (~20–22°C), and continuously bubbled with O_2/CO_2 (95/5%). Micropipettes with 12–14 MΩ resistance (tip inner diameter: 1.00 ± 0.13 μm, outer diameter: 1.82 ± 0.14 μm; means ± SD, n=5) were constructed from borosilicate glass (1 mm OD, 0.5 mm ID) using a P97 pipette puller (Sutter Instruments, Novato, CA) and filled with an enzyme reaction mixture or lactate or glucose solutions. The osmolarity of each solution was measured (Osmette II, Precision Systems, Natick MA) and adjusted to 300–310 mOsm/L with sucrose. Neurons and astrocytes in brain slices were visualized under infrared-differential interference contrast (IR-DIC) (Dodt and Zieglgänsberger, 1990) with a Nikon Eclipse E600 microscope (Melville, NY) using a Photometrics CoolSNAP ES camera (Roper Scientific, Atlanta, GA) and MetaVue software (Molecular Devices, Sunnyvale, CA). Cells were impaled with micropipettes using a MP-225 manipulator (Sutter Instruments, San Francisco, CA) and material allowed to diffuse into cells. Fluorescence intensity and labeled areas were determined with MetaVue software.

Single-cell, fluorescence-linked enzyme assays for lactate and glucose

Conversion of lactate to pyruvate by lactate oxidase from *Pediococcus sp*. consumes O_2 and generates H_2O_2, which was measured quantitatively by horseradish peroxidase-catalyzed oxidation of non-fluorescent Amplex red to fluorescent resorufin. Resorufin (Invitrogen-Molecular Probes, Carlsbad, CA) standard curves were freshly prepared from a 10 mmol/L stock solution dissolved in DMSO and diluted in 50 mM Tris-HCl, pH 7.4. The lactate reporter system contained Amplex red (200 μmol/L; Molecular Probes), lactate oxidase (4 units/ml; E.C. number, 1.13.12.4; Sigma-Aldrich, catalog number L0638), and horseradish peroxidase (0.8 units/ml; E.C. 1.11.1.7, Sigma-Aldrich, P2088) in 50 mmol/L Tris-HCl, pH 7.4, that was

previously deoxygenated with helium to minimize spontaneous oxidation of Amplex red. L-lactate and D-glucose dilutions were prepared fresh daily in 50 mmol/L Tris-HCl, pH 7.4. Cellular glucose uptake and intercellular transfer was measured using the conversion of D-glucose to glucono-1,5-lactone by glucose oxidase and coupling this reaction to the oxidation of non-fluorescent Amplex red to fluorescent resorufin by horseradish peroxidase. The glucose reporter system contained Amplex red (200 μmol/L), glucose oxidase (1 unit/ml; E.C. 1.1.3.4, Sigma-Aldrich, G7141, *Aspergillus niger*), and horseradish peroxidase (1 unit/ml) in deoxygenated 125 mmol/L Tris-HCl, pH 7.4.

Statistics

All statistical analyses were performed with GraphPad Prism® software, version 5.02 (GraphPad Software. La Jolla, CA). Comparisons between two groups of independent samples were made with two-tailed, unpaired t tests. Comparisons among 3 or more groups of independent samples were made with one-way ANOVA and Tukey's test. $P<0.05$ was considered to be statistically significant.

RESULTS

A sensitive, specific, real-time enzymatic fluorescent assay to measure lactate in single cells

The coupled reaction utilizing lactate oxidase, horseradish peroxidase, and Amplex red oxidizes L-lactate and generates resorufin, a fluorescent compound (Fig. 1a, left panel) with a 1:1 stoichiometry for lactate oxidation and resorufin formation (Fig. 1a, right panel). Thus, diffusion of this reaction mixture into a neuron or astrocyte via a micropipette would enable quantitative assays of lactate uptake from extracellular fluid into astrocytes and neurons (Fig. 1b, Scheme 1, blue), shuttling of lactate from an astrocyte to a neuron (Fig. 1b, Scheme 2, green), and trafficking of lactate among gap junction-coupled astrocytes (Fig. 1b, Scheme 3, red).

Putative neurons and astrocytes in slides of adult rat inferior colliculus were identified by their morphology and dye-labeling characteristics because use of sulforhodamine 101 to identify astrocytes in slices of inferior colliculus (Ball et al., 2007) would interfere with resorufin fluorescence assays. Neurons with 10–12 μm diameter cell bodies and clearly identifiable processes were visualized (Fig. 2a) under infrared differential interference (IR-DIC) contrast microscopy, then impaled with a micropipette containing 4% Lucifer yellow VS (LYVS); dye diffusion labeled the soma and processes of a single cell (Fig. 2b). In contrast, IR-DIC visualization (Fig. 2c) and dye-labeling of astrocytes identified nuclear (Fig. 2d) and cytoplasmic labeling of many gap junction-coupled cells plus perivascular labeling (Fig. 2e), which coregisters with an astrocytic marker (Ball et al., 2007). Labeling of putative neurons rarely involved more than one cell (i.e., arising from cellular damage by the micropipette), whereas putative astrocytes were dye-coupled with perivascular labeling. Diffusion of the enzymatic reporter system into a neuron and placement of a lactate-containing micropipette outside the cell caused a small increase in fluorescence within the cell and its processes during a 5 min interval (Fig. 2f, g) whereas the fluorescence response was much greater in astrocytes (Fig. 2h, i). These assays provide proof of principle that fluorescent enzymatic assays carried out in single cells in adult brain slices can be used to assay lactate.

To establish quantitative conditions for assay of intracellular lactate concentration, the linear intracellular fluorescence range for resorufin was determined by constructing standard curves in neurons and astrocytes in brain slices with known concentrations of authentic resorufin. When single astrocytes were impaled with micropipettes containing 20 or 40 μmol resorufin/L and resorufin fluorescence repeatedly measured over a 5 min experimental interval, the change in fluorescence above baseline (ΔF) was stable with time and proportional to

concentration (Fig. 3a). To minimize leakage from cells, the micropipette was not removed from the reporter cell after enzyme insertion, and any effects of photobleaching were minimal due to dye diffusion between the cell and the micropipette. Next, resorufin fluorescence was shown to be identical in neurons and astrocytes and linear over the range 0–50 μmol resorufin/L (Fig. 3b) but not at higher resorufin levels (Fig. 3b, inset). Gap junction permeability of resorufin may interfere with comparisons of lactate levels in coupled astrocytes and non-coupled neurons due to its diffusion from the reporter astrocyte into the syncytium, but when assayed directly by simultaneous diffusion of resorufin and Lucifer yellow VS into single astrocytes, the resorufin did not label other cells, whereas Lucifer yellow quickly spread through the syncytium, labeling a large area (Fig. 3c,Fig. 2e). When lactate uptake from an extracellular point source was tested (Fig. 1b, Scheme 1, blue), the resorufin generated by lactate uptake from a micropipette located either 2 or 50 μm from the astrocyte was 2.5 times higher than that into neurons (Fig. 3d). Taken together, these results validate the novel use of a coupled enzymatic reaction to assay intracellular lactate levels by demonstrating that the resorufin signal is stable, equivalent in both major brain cell types, linear over a defined range, localized only to the cell containing the enzymes, and neurons and astrocytes in situ are differentially responsive to the same level of extracellular lactate.

Lactate uptake into astrocytes and neurons from extracellular fluid

Cellular lactate transport rates and capacities were assessed by determination of the concentration dependence of lactate uptake into astrocytes and neurons in non-stimulated slices of adult rat inferior colliculus over the range from the average lactate level in activated tissue to levels above the highest K_m value for lactate for brain monocarboxylic acid transporters (MCT). Raising extracellular lactate concentration in a micropipette adjacent to astrocytes from 2 to 40 mmol/L (Fig. 4a) progressively increased the initial, linear rise in resorufin fluorescence (ΔF) during the first 60 s and the plateau value during the 240–300 s interval. The plateau is denoted as net uptake, and is assumed to reflect the apparent steady state between lactate uptake into the cell, generation of resorufin by the enzymatic reporter system, and diffusion of resorufin into the pipette. Cellular lactate transport capacity is considered to be the factor determining net uptake because the enzymatic activity and rate of diffusion into the micropipette are independent of cell type. Mechanical perturbation of astrocytes is known to induce intracellular calcium waves and is likely to cause an endogenous metabolic response. However, the contribution endogenously-produced lactate was small in two control assays, i.e., (i) after insertion of the enzyme-containing micropipette into a cell with no extracellular pipette, or (ii) insertion of the reporter system into a cell and placement of a second, buffer-containing (denoted as 0 lactate) pipette outside of a cell; these low values were not subtracted from lactate uptake values (Fig. 4a, b). These control assays also demonstrate a requirement for provision of exogenous lactate outside of cell for a response.

Lactate concentration-dependent profiles were also obtained in neurons (Fig. 4b) but they had lower initial rates and final values compared to astrocytes. In both cell types, the initial lactate uptake rate was linear with respect to lactate concentration (Fig. 4c, d), but it was much faster in astrocytes compared to neurons (Fig. 4d, inset), even at 2 mmol/L lactate (Fig. 4c, inset), which approximates tissue lactate levels in rat and human brain during physiological activation. The apparent lack of saturation of the neuronal lactate transporter MCT2 (Fig. 4b, d) was unexpected due to its low K_m (~0.7 mmol/L; Manning Fox et al., 2000), and was probably due to diffusion of lactate from the micropipette along the cell surface so that more transporters contributed to lactate uptake at higher compared to lower concentrations and increased the apparent K_m. Astrocytic MCT1 and MCT4 have higher K_m's for lactate (~ 4 and ~28 mmol/L, respectively; Manning Fox et al., 2000), and MCT4 would not be saturated at 40 mmol/L, so any effects of diffusion and transporter number would be less evident. Net uptake of lactate into astrocytes also exceeded that into neurons over the entire range (Fig. 4e, f, insets).

Extracellular lactate is most likely to be taken up by astrocytes even at 2 mmol lactate/L (i.e., the mean level in activated brain) due to their 4.3-fold faster and 2.3-fold higher-capacity compared to neurons.

Lactate trafficking from astrocyte to astrocyte and astrocyte to neuron

Increased concentrations of extracellular lactate inhibit lactate production from glucose with apparent K_i values of 0.5 and 3.5 mmol/L in cultured astrocytes and neurons, respectively (Ramírez et al., 2007; Rodrigues et al., 2009), indicating that rapid removal of lactate from activated intracellular domains is essential to maintain a high glycolytic rate during cellular activation. Transfer of lactate from one gap junction-coupled astrocyte to another was, therefore, tested directly (Fig. 1b, Scheme 3, red) by diffusing Lucifer yellow plus the reaction mixture into a single astrocyte to identify coupled cells, then inserting a lactate-filled micropipette into a dye-coupled astrocyte located about 50 μm from the enzyme-loaded reporter cell. Astrocyte-to-astrocyte lactate transfer rate and amount increased with intracellular lactate level (Fig. 5a), and is representative of simultaneous lactate transfer among the many astrocytes coupled to the donor cell. The equivalent lactate uptake into astrocytes at 2 and 50 μm from the pipette (Fig. 3d) may reflect lactate trafficking among coupled astrocytes after its uptake into cells near the source.

Lactate transporters are active during the shuttling assays, some lactate would be released from astrocytes and may be taken up by other astrocytes (Fig. 4), as well as by nearby neurons (Fig. 1b, Scheme 2, green). Shuttling of lactate from an astrocyte to a neuron located about 50 μm away from the donor cell was detectable but it exhibited modest concentration dependence (Fig. 5b) and was much lower than trafficking among astrocytes (Fig. 5a). The initial rate of lactate diffusion between two coupled astrocytes increased with lactate level between 0–5 mmol/L, whereas the rate of lactate transfer from an astrocyte to a neuron did not vary with lactate level in the donor astrocyte over the range 2–10 mmol lactate/L (Fig. 5c). Dispersion of lactate among coupled astrocytes and relatively slow transport into neurons compared to astrocytes (Figs. 4c, d) with washout of extracellular lactate from the slice probably contributed to lack of concentration dependence of astrocyte-to-neuron transfer. Net transfer of lactate between two astrocytes was 4.9 times greater from an astrocyte to a neuron located the same distance from the source cell (Fig. 5d), demonstrating that the capacity for lactate transfer within the astrocytic syncytium vastly exceeds local shuttling from astrocytes to neurons. Note that overall intercellular trafficking among astrocytes includes gap junctional communication plus release to extracellular fluid and re-uptake into the same or coupled astrocytes comprising the syncytium. Gap junction dependence of lactate trafficking among astrocytes was verified by octanol treatment; this gap junction blocker reduced lactate dispersal by ~75% (Fig. 5 legend).

Glucose transfer from astrocytes to neurons

Failure to detect transfer of the fluorescent glucose analog, 2-NBDG, from an astrocyte to neighboring neuron in hippocampal slices from immature mice (Rouach et al., 2008) was surprising because glucose transporters are abundant in neurons and astrocytes (Simpson et al., 2007). Because diffusion of glucose between brain cells and interstitial fluid should enable astrocytes to provide glucose to nearby neurons, we directly tested this notion by devising a resorufin-based, single-cell assay for glucose uptake and shuttling. Glucose transport into neurons from an extracellular point source containing 20 mmol glucose/L (Fig. 6a) and from a nearby astrocyte (Fig. 6b) was readily detected and was blocked by cytochalasin B, a glucose transport inhibitor. Initial rates of glucose uptake (Fig. 6c) and net glucose uptake (Fig. 6d) into neurons directly from extracellular fluid and from astrocytes (via extracellular fluid) were similar in magnitude indicating that glucose can be supplied to neurons from astrocytes. Mean changes in resorufin fluorescence elicited by uptake and diffusion (Fig. 4–Fig. 6) were within

the linear range (Fig. 3b), but the lactate and glucose enzymatic assay systems were not cross-calibrated, so their absolute transport values cannot be directly compared.

DISCUSSION

Methodological considerations and transport estimates

A novel approach was developed to assay quantitatively the intracellular levels of lactate and glucose and this technique was used to reveal high lactate transport capacity in astrocytes compared to neurons and the ability of astrocytes to provide glucose to neurons. Real-time lactate oxidase-coupled fluorometric assays have high sensitivity and selectivity, 1:1 stoichiometry, adequate linear range, and very low resorufin gap junction permeability. As shown with glucose oxidase, this approach is readily adapted for quantitative determination of levels of a wide range of non-derivatized, endogenous compounds in brain cells within the complex 3-dimensional environment of adult brain slices. Assays of metabolite transfer into single cells or between coupled and neighboring cells are technically difficult because two micropipettes must be inserted into tissue within close proximity and assays are limited to a few cells, contrasting the single cell and population assays that can be carried out with membrane-permeant fluorescent compounds. The pipette components (enzymes, test substrates, and buffer) will overwhelm the endogenous metabolic activities in the test cells because the fluid volume of the micropipette is infinite compared to that of cells (e.g., 66,000 μm^3 or 66 pL for the average protoplasmic astrocyte in adult CA1 hippocampus, Bushong et al., 2002), and soluble compounds and enzymes will diffuse into the pipette and reduce interference. Autofluorescence by cellular NADH and FAD is low due to dilution and their respective absorbance (340 and 450 nm) and fluorescence emission (460 and 525 nm) maxima compared to resorufin (563 and 587 nm; Zhou et al., 1997). Endogenous catalase could reduce the signal by consuming H_2O_2 produced by the oxidase, but product loss should have the greatest effect at lowest rates and cause non-linearity at the lower end of the rate plots; this was not observed (Fig. 4), supporting the likelihood that the activities of the reporter enzymes greatly exceed endogenous activities. Lactate transport exhibits pH dependence but this effect would be minimal due to the same pH in the donor and reporter pipette buffers. Brain slice assays cannot eliminate endogenous extracellular metabolites, causing uncertainty in the true substrate concentration when test levels are near or below that in tissue, in contrast to in vitro transport studies with isolated cells that can test a wide range of uniform extracellular substrate levels. In slices, spreading from the point source at higher substrate levels may result in (i) an increased number of transporters in the reporter cell that contribute to substrate uptake, thereby raising apparent K_m, and (ii) increased number of astrocytes may take up substrate and deliver it to the reporter cell via gap junctions, thereby overestimating single-cell uptake; patch clamping and gap junction blockers could be used to minimize these issues.

Technical limitations do not allow transporter K_m and T_{max} (maximal transport rate that is proportional to transporter number, analogous to V_{max} for enzymes) determination in the present study, but oxidase-based assays revealed greater lactate transport rates and capacity in astrocytes compared to neurons that have matured within the context of normal development, cell-cell interactions, and function in the inferior colliculus. Based on known MCT K_m values (Manning Fox et al., 2000; see Fig. 7), neuronal MCT2 would be operating at 94–97% of T_{max} at 10–20 mmol/L lactate and measured rates at these concentrations (i.e., 2–4 ΔF/s, Fig. 4d), therefore, reflect transporter number. In contrast, astrocytic MCT1 and MCT4 would be 91 and 59% of the respective T_{max} at 40 mmol/L, and, depending on the relative proportion of MCT1 and MCT4 transporters, the composite astrocyte T_{max} may range from 1–2 times the measured rate at 40 mmol/L (i.e., 32.8 – 65.6 ΔF/s, Fig. 4c). Thus, MCT1/4 transporter number in astrocytes may be as high as 8–33 times that of neurons (calculated from the above ranges of ΔF/s), assuming the catalytic capacity (k_{cat}) per transporter is the same for all isoforms

(Simpson et al., 2007). Calculations using simple Michaelis-Menten kinetics (i.e., $v = (T_{max} S)/(Km + S)$) and T_{max} values at the boundaries of the ranges for neurons (2–4) and astrocytes (33–66) and different proportions of MCT1 and MCT4 (25/75, 50/50, 75/25) suggest that when the boundary values favor neurons (i.e., $T_{max}^{neuron} = 4$; $T_{max}^{astrocyte} = 33$) 48–55% of the extracellular lactate may be taken up into neurons in 'resting' brain when lactate levels are 0.5–1 mmol/L; this fraction falls to 40 and 30% during activation if lactate levels are 2 and 5 mmol/L, respectively, and progressively decreases to lower values as lactate levels rise further. On the other hand, when the boundary values favor astrocytes ($T_{max}^{neuron} = 2$; $T_{max}^{astrocyte} = 66$), only 19–24% of the extracellular lactate may be taken up into neurons when lactate levels are 0.5–1 mmol/L; this fraction falls to 14 and 10% at 2 and 5 mmol/L, respectively, and declines to lower values as lactate levels rise further. It must be emphasized that above values derived from these calculations are rough estimates that are not as accurate as desired. However, they support the notion that astrocytes take up most of the extracellular lactate during activation and ~45–75% during resting conditions.

The resorufin standard curves measured in astrocytes and neurons (Fig. 2) and measured cellular lactate uptake rates (Fig. 3) can be used to convert uptake rates from ΔF/s to μmol/L/s (i.e., per unit cellular volume). For example, at 2 mmol/L lactate, uptake rates in astrocytes and neurons are 0.04 an 0.01 μmol/L/s, respectively. If one assumes that neurons and astrocytes in the inferior colliculus have volumes similar to that of hippocampal protoplasmic astrocytes (i.e., 66 pL; Bushong et al., 2002), the corresponding rates per cell are 2.7 and 0.8×10^{-15} mmol/s, respectively; estimated T_{max} values are 1.1–2.2 and 0.05–0.15 μmol/L/s (or 75–145×10^{-15} and 4–8.5×10^{-15} mmol/s) for astrocytes and neurons, respectively. Within the context of limitations of the present study noted above, these estimated T_{max} values are at least 7-fold (and up to 30–40-fold) higher for astrocytes than neurons, sharply contrasting the approximately 4:1 neuron-to-astrocyte ratio for MCT T_{max} used in recent modeling studies of cellular glucose utilization and lactate production (Aubert and Costalat, 2005;Aubert et al., 2007;Simpson et al., 2007;Mangia et al., 2009b). These results emphasize the need for further in vivo studies to establish cellular MCT transporter numbers, identify cells that produce lactate during activation, establish regional differences in these variables (e.g., transporter number would be expected to vary with demands of regional metabolic rate), and determine the range of actual lactate levels in activated glycolytic microdomains. The likelihood of heterogeneous brain lactate levels in small compartments with high concentrations that exceed the average tissue value of about 2 mmol/L is supported by release of lactate from brain to blood when average brain lactate levels are less than those in blood (see Table 1 in Dienel and Cruz, 2003).

Lactate generation, shuttling, and release

The combination of two key characteristics of brain cells is likely to underlie clearance of extracellular lactate via astrocytes when it is produced within brain cells at high local rates during acute activation regardless of the cellular origin of lactate, (i) the higher K_m values for astrocytic MCT1 and MCT4 lactate transporters compared to neuronal MCT2, and (ii) higher maximal lactate transport capacity (T_{max}) compared to maximal lactate oxidation capacity (V_{max}) in brain cells. When local lactate levels rise above the normal value of ~0.5–1 mmol/L, MCT2 becomes saturated at lower levels than MCT1 and MCT4, blunting the increase in neuronal lactate transport rate compared to that in astrocytes (Fig. 7c, table). The 4.3-fold faster and 2.3-fold greater net lactate transport into astrocytes compared to neurons in adult brain slices (Fig. 4) is consistent with a much higher T_{max} in astrocytes, as discussed above. Isolated nerve endings (synaptosomes) from adult rat brain have a 5-fold higher T_{max} compared to V_{max} for lactate (McKenna et al., 1998), and in tissue culture, astrocytes have higher lactate transport rates than neurons, but the rate of net lactate uptake, which is metabolism-driven, is much lower than transport rate and similar in these two cell types (reviewed by Dienel and

Hertz, 2001). Thus, when intracellular and extracellular lactate levels equilibrate, excess lactate can diffuse down its concentration gradients through interstitial fluid and astrocytic syncytia to endfeet, perivascular fluid, and blood for clearance (Fig. 7c). Lactate release and use by other tissues during 'overflow' conditions is not a waste of energy-rich fuel because brain glucose supply normally closely matches local demand and glucose and lactate transport are equilibrative processes.

Metabolic modeling of glucose and lactate transport and utilization has predicted that glucose is consumed mainly in neurons, activation-induced lactate transients are generated in neurons, and lactate is shuttled from neurons to astrocytes (Simpson et al., 2007; Mangia et al., 2009b). In fact, neuronal synaptic endings are capable of up-regulating glycolysis and oxidative metabolism many-fold during activating conditions, and they can maintain a 10-fold rise in glycolytic rate for 30 min (Kauppinen and Nicholls, 1986). Furthermore, two recent studies of regulation of mitochondrial metabolism by calcium proposed a mechanism for neuronal lactate production during brain activation (Bak et al., 2009; Contreras and Satrústegui, 2009). In brief, activity-induced increased Ca^{2+} entry into mitochondria enhances tricarboxylic acid cycle flux and limits the availability of α-ketoglutarate to participate in the malate-aspartate shuttle, the system that transfers reducing equivalents from cytoplasmic NADH into mitochondria; accumulation of cytoplasmic NADH would then drive lactate production in activated neurons to maintain increased glycolysis (Bak et al., 2009; Contreras and Satrústegui, 2009). The possibility that lactate generation in activated brain is *independent* of astrocytic glutamate transport (as observed in a number of studies in cultured astrocytes; see Tables 5 and 6 in Dienel and Cruz, 2004; Fig 2 and Fig 3, Dienel and Cruz, 2006) is supported by an in vivo study in cerebellum (Caesar et al., 2008) using CNQX, a postsynaptic AMPA receptor blocker that does not impair glutamate-stimulated glucose utilization in cultured astrocytes (Pellerin and Magistretti, 1994). CNQX prevented the stimulus-induced rise in postsynaptic activity, the increase in rates of blood flow and oxygen and glucose utilization, and the rise in extracellular lactate level (Caesar et al., 2008). Together, data in this and the above studies challenge the widely-accepted notion of the cellular origin of lactate (i.e., neurons instead of astrocytes), the direction of lactate shuttling (i.e. neuron to astrocyte instead of astrocyte to neuron), and dissociate the rise in fuel consumption and lactate production from glutamate transport; they support the model describing rapid release of lactate from activated brain instead of its utilization as a major fuel in normal subjects during brain activation Fig. 7.

Lactate trafficking may involve some lactate use as fuel by neurons and astrocytes, both of which can oxidize lactate in adult rat brain (Zielke et al., 2009). Net lactate production within brain is not known, but, during resting conditions when the oxygen/glucose metabolic ratio is close to 6, small amounts of lactate are released to blood. During brain activation, lactate production is anticipated to rise but the overall contribution of endogenously-generated lactate to energetics is probably small compared to that of glucose. In metabolic labeling studies using [1- and 6-^{14}C]glucose, local pyruvate/lactate oxidation would lead to incorporation of label into the tricarboxylic acid cycle-derived amino acid pools, and the rise in accumulation of total labeled metabolites in tissue of ~15–25% in brain activation studies (see Introduction) defines an upper limit for increased 'direct' oxidation of glucose-derived pyruvate plus utilization of lactate provided by cell-to-cell shuttling from glycolytic to oxidative domains. This estimate is similar to the small (~10%) rise in phosphorylation of NBDG, a fluorescent glucose analog, in neurons but not astrocytes during blockade of MCT2 with 100 μmol/L α-cyano-4-hydroxy-cinnamate (4-CIN) in brainstem chemosensory regions (Erlichman et al., 2008). Part of this compensatory response to MCT blockade may have arisen from reduced transport of glucose-derived pyruvate into mitochondria by 4-CIN, which potently inhibits pyruvate oxidation in mitochondria isolated from brain and other tissues; in heart mitochondria, the K_i for pyruvate transport is 1–6 μmol/L, with nearly complete inhibition of pyruvate-dependent O_2 uptake at 100 μmol/L (Halestrap, 1975; Halestrap and Denton, 1974, 1975). To summarize, metabolic,

transport, and modeling studies support the likelihood of faster transport-mediated lactate trafficking and release from activated tissue compared to its local metabolism during activating conditions. There are, however, circumstances when exogenous lactate serves as a significant brain fuel, such as when its blood concentration rises to very high levels during severe exercise (van Hall et al., 2009).

Functional anatomy links transport, syncytial network trafficking, and energetics

The astrocytic syncytium represents a multi-cellular network with many cellular and subcellular compartments that can be linked together or separated by regulation of gap junctional connectivity. Because the goal of the present study was to compare overall astrocytic and neuronal lactate trafficking from point sources or from single source cells, assays were carried out in the absence of octanol so that contributions of coupled cells to the response of the reporter cell could be registered as reflecting the total, local astrocytic capacity during brain functional activity. For example, the large volume of the average protoplasmic astrocyte and its extensive arbor of its fine filopodial processes that surround neurons (Bushong et al., 2002) could greatly increase the surface area for glucose delivery from a single astrocyte via many gap junction-coupled astrocytes to a nearby neuron compared to the small cross-section area of the 1 μm diameter micropipette used for focal application of glucose to a neuron (Fig. 6). Note that cell-to-cell transfer distances were measured in our studies but the actual path length traveled by substrates and dyes is not known and may involve various transcellular routes. Another important factor relevant to astrocyte-to-neuron glucose trafficking is the high glucose transport capacity of neurons; it is estimated to be at least 9 times that of astrocytes at 5 mmol/L glucose due to kinetic differences between the neuronal GLUT3 (K_m 2.8 mmol/L, k_{cat} = 6,512/sec) and the astrocytic GLUT1 (K_m = 8 mmol/L; k_{cat} = 1,166/sec) glucose transporters (Simpson et al., 2007). The large surface area of astrocyte-neuron interactions, different K_m's for the respective GLUTs, high glucose level (20 mmol/L) in the micropipette, and avid neuronal uptake of extracellular glucose released from astrocytes may explain the similar glucose uptake rates from a pipette and a more distant astrocyte (Fig. 6). The influence of syncytial trafficking to neuronal glucose uptake and to astrocytic lactate dispersal could be tested in future assays in the presence of octanol.

Astrocytes in the inferior colliculus are highly gap junction coupled, providing extensive intracellular routes that are linked to interstitial fluid via transporters and to perivascular fluid via their endfeet. Syncytial distribution capacity for fuel, metabolites, electrolytes, neurotransmitter precursors, and by-products can be visualized by dye spread (Ball et al., 2007; Rouach et al., 2008) from a single astrocyte to thousands other astrocytes (Fig. 7a) and their perivascular endfeet at some distance from the impaled cell (Fig. 7b). The rapid, high-capacity lactate transport system in astrocytes probably involves diffusion through gap junctions as well as uptake, release, and re-uptake via transporters; in the intact brain this transmembrane substrate 'cycling' process would be more extensive than in slices where extracellular material can be washed out into the perfusion solution. In fact, substrate release and washout does affect dye-labeled area in cultured astrocytes; we found that omission of a glucose transporter inhibitor reduced the area labeled by the fluorescent glucose analog 2-NBDG by 56% (see Table 1 in Gandhi et al., 2009). A physiological advantage of gap junctional communication plus transmembrane substrate cycling is that extracellular diffusional limitations imposed by dead-space microdomains (Hrabetová and Nicholson, 2004) can be circumvented. Fig. 7c illustrates the concept of preferential astrocytic uptake of lactate generated by glycolytically-activated neurons or astrocytes, lactate cycling across membranes, and distribution of lactate to endfeet where it can be released to perivascular fluid, dispersed along the vasculature, and ultimately released to venous blood. This pathway may enable rapid channeling and preferential release of glucose-derived lactate during brain activation; minimal use of labeled and unlabeled lactate as an oxidative fuel would explain the large underestimates

of glucose utilization with [^{14}C]glucose (see Introduction). An intriguing implication of astrocyte-mediated trafficking of lactate along the vasculature (Fig. 7c) is that lactate can modulate blood flow (Laptook et al., 1988; Yamanishi et al., 2006; Gordon et al., 2008), and large syncytia may enable astrocyte-mediated blood flow regulation in a larger tissue volume than that of metabolically-activated cells, thereby helping ensure fuel delivery and by-product removal in excess of demand.

Emerging evidence supports the importance of astrocytic syncytial networks for neuron-astrocyte metabolic interactions (Giaume and McCarthy, 1996; Cruz et al., 2007; Ball et al., 2007; Rouach et al., 2008; Tabernero et al., 1996, 2006; Stout et al., 2009; and references cited in these studies), but network metabolite fluxes are not known and some results of syncytial trafficking studies appear to be discordant. For example, we found that astrocytic gap junctional passage of three hexose-6-phosphates is highly restricted compared to anionic fluorescent dyes, hexoses, a triose-phosphate, NADH, and NADPH (Gandhi et al., 2009), whereas Barros et al. (2009) provide evidence for transfer of 2-NBDG-6-P (a fluorescent glucose analog) in cerebellum. The apparent gap junctional permeability of [^{14}C]glucose-6-P in scrape-load assays that measured ^{14}C-labeled area (Tabernero et al., 1996, 2006) probably arose from metabolism of [^{14}C]glucose-6-P by enzymes released from cells damaged by scrape-loading, enabling diffusion of unidentified downstream, gap junction-permeable [^{14}C]metabolites. The importance of astrocyte-to-neuron lactate trafficking in hippocampal slices from 2–4 week-old mice was inferred (Rouach et al., 2008) from (i) apparent lactate-dependence of synaptic transmission during assays in the presence of 200 μmol/L 4-CIN and (ii) undetectable astrocyte-to-neuron transfer of 2-NBDG, suggesting that glucose is not passed on to astrocytes and lactate shuttling is necessary to fuel neurons. As noted above, 200 μmol/L 4-CIN completely blocks pyruvate transport and oxidation in isolated mitochondria (Halestrap, 1975; Halestrap and Denton, 1974, 1975), and in cultured neurons 250 μmol/L 4-CIN reduces lactate and glucose oxidation to 13% and 42% of control rates, respectively (McKenna et al., 2001). Thus, reduced oxidation of glucose-derived pyruvate may have contributed to impairment of synaptic transmission by 4-CIN (Rouach et al., 2008). We observed robust astrocytes-to-neuron glucose shuttling in adult brain slices (Fig. 6) under conditions that favor its detection, i.e., by diffusion of a high concentration of glucose (20 mmol glucose/L) into a single astrocyte; this level would overwhelm its metabolism by endogenous hexokinase and create a strong concentration gradient from the source cell. Further work is necessary to evaluate astrocyte-to-neuron glucose trafficking at lower, normal brain glucose levels and during high neuronal glucose demand, but proof of principle is established. Also, these results suggest that the sensitivity of the 2-NBDG transfer assay, regional differences (i.e., inferior colliculus has higher metabolic rate than hippocampus and would require high, matching transport capacity), and animal age may have contributed to these apparently-discrepant results in 2–4-week-old and adult animals. Large, developmental changes in the number, cellular, and regional distributions of brain glucose and lactate transporters, levels of metabolic enzymes, and substrates used for brain fuel (i.e., a shift from utilization of ketones, lactate, and glucose during the suckling period to glucose after weaning (Cremer, 1982; Vannucci and Simpson, 2003)), must be taken into account in studies using cultured cells and tissue from immature animals. Although brain slices have the complex architecture of the brain, they incur preparative damage and lack blood flow. Because arterial pulsations power perivascular fluid flow and tracer distribution in brain (Rennels et al., 1985) metabolite spreading and release from living brain is expected to exceed that in slices. Furthermore, disease states that cause vascular basement membrane thickening (e.g., diabetes and cerebrovascular disease) or blockade of perivascular flow (e.g., Alzheimer's disease with amyloid plaques in perivascular space) could interfere with fuel distribution within brain and lactate clearance in vivo, thereby influencing brain energetics and interpretation of brain imaging and spectroscopic studies.

Abbreviations used

aCSF, artificial cerebrospinal fluid; MCT, monocarboxylic acid transporter; 4-CIN, α-cyano-4-hydroxy-cinnamate; 2-NBDG, 2-(*N*-(7-nitrobenz-2-oxa-1,3-diazol-4-yl)amino)-2-deoxyglucose; LYVS, Lucifer yellow VS; IR-DIC, infrared differential interference contrast.

Acknowledgments

This work was supported by National Institutes of Health grants NS36728 and NS47546, Alzheimer Foundation grant IIRG-06-26022, and the University of Arkansas for Medical Sciences Department of Physiology & Biophysics, Graduate School, and Research Council.

REFERENCES

Ackermann RF, Lear JL. Glycolysis-induced discordance between glucose metabolic rates measured with radiolabeled fluorodeoxyglucose and glucose. J. Cereb. Blood Flow Metab 1989;9:774–785. [PubMed: 2584274]

Adachi K, Cruz NF, Sokoloff L, Dienel GA. Labeling of metabolic pools by [6-^{14}C]glucose during K^+-induced stimulation of glucose utilization in rat brain. J. Cereb. Blood Flow Metab 1995;15:97–110. [PubMed: 7798343]

Aubert A, Pellerin L, Magistretti PJ, Costalat R. A coherent neurobiological framework for functional neuroimaging provided by a model integrating compartmentalized energy metabolism. Proc. Natl. Acad. Sci. U. S. A 2007;104:4188–4193. [PubMed: 17360498]

Aubert A, Costalat R. Interaction between astrocytes and neurons studied using a mathematical model of compartmentalized energy metabolism. J. Cereb. Blood Flow Metab 2005;25:1476–1490. [PubMed: 15931164]

Bak LK, Walls AB, Schousboe A, Ring A, Sonnewald U, Waagepetersen HS. Neuronal glucose but not lactate utilization is positively correlated with NMDA-induced neurotransmission and fluctuations in cytosolic Ca^{2+} levels. J. Neurochem 2009;109:87–93. [PubMed: 19393013]

Ball KK, Gandhi GK, Thrash J, Cruz NF, Dienel GA. Astrocytic connexin distributions and rapid, extensive dye transfer via gap junctions in the inferior colliculus: Implications for [^{14}C]glucose metabolite trafficking. J. Neurosci. Res 2007;85:3267–3283. [PubMed: 17600824]

Barros LF, Courjaret R, Jakoby P, Loaiza A, Lohr C, Deitmer JW. Preferential transport and metabolism of glucose in Bergmann glia over Purkinje cells: a multiphoton study of cerebellar slices. Glia 2009;57:962–970. [PubMed: 19062182]

Bergersen LH. Is lactate food for neurons? Comparison of monocarboxylate transporter subtypes in brain and muscle. Neuroscience 2007;145:11–19. [PubMed: 17218064]

Bushong EA, Martone ME, Jones YZ, Ellisman MH. Protoplasmic astrocytes in CA1 stratum radiatum occupy separate anatomical domains. J. Neurosci 2002;22:183–192. [PubMed: 11756501]

Caesar K, Hashemi P, Douhou A, Bonvento G, Boutelle MG, Walls AB, Lauritzen M. Glutamate receptor-dependent increments in lactate, glucose and oxygen metabolism evoked in rat cerebellum in vivo. J. Physiol 2008;586:1337–1349. [PubMed: 18187464]

Cerdán S, Rodrigues TB, Sierra A, Benito M, Fonseca LL, Fonseca CP, García-Martín ML. The redox switch/redox coupling hypothesis. Neurochem Int 2006;48:523–530. [PubMed: 16530294]

Chih CP, Roberts EL Jr. Energy substrates for neurons during neural activity: a critical review of the astrocyte-neuron lactate shuttle hypothesis. J. Cereb. Blood Flow Metab 2003;23:1263–1281. [PubMed: 14600433]

Collins RC, McCandless DW, Wagman IL. Cerebral glucose utilization: Comparison of [^{14}C] deoxyglucose and [6-^{14}C]glucose quantitative autoradiography. J. Neurochem 1987;49:1564–1570. [PubMed: 3668540]

Contreras L, Satrústegui J. Calcium signaling in brain mitochondria: interplay of malate aspartate NADH shuttle and calcium uniporter/mitochondrial dehydrogenase pathways. J. Biol. Chem 2009;284:7091–7099. [PubMed: 19129175]

Cremer JE. Substrate utilization and brain development. J. Cereb. Blood Flow Metab 1982;2:394–407. [PubMed: 6754750]

Cruz NF, Adachi K, Dienel GA. Metabolite trafficking during K^+-induced spreading cortical depression: Rapid efflux of lactate from cerebral cortex. J. Cereb. Blood Flow Metab 1999;19:380–392. [PubMed: 10197508]

Cruz NF, Ball KK, Dienel GA. Imaging focal brain activation in conscious rats: Metabolite spreading and release contribute to underestimation of glucose utilization with [^{14}C]glucose. J. Neurosci. Res 2007;85:3254–3266. [PubMed: 17265468]

Dienel GA, Cruz NF. Neighborly interactions of metabolically-activated astrocytes in vivo. Neurochem. Int 2003;43:339–354. [PubMed: 12742078]

Dienel GA, Cruz NF. Nutrition during brain activation: does cell-to-cell lactate shuttling contribute significantly to sweet and sour food for thought? Neurochem. Int 2004;45:321–351. [PubMed: 15145548]

Dienel GA, Cruz NF. Astrocyte activation in working brain: energy supplied by minor substrates. Neurochem. Int 2006;48:586–595. [PubMed: 16513214]

Dienel GA, Cruz NF. Imaging Brain Activation: Simple Pictures of Complex Biology. Ann. N. Y. Acad. Sci 2008;1147:139–170. [PubMed: 19076439]

Dienel GA, Cruz NF. Exchange-mediated dilution of brain lactate specific activity: Implications for the origin of glutamate dilution and the contributions of glutamine dilution and other pathways. J. Neurochem 2009;109:30–37. [PubMed: 19393006]

Dienel GA, Hertz L. Glucose and lactate metabolism during brain activation. J. Neuroscience Res 2001;66:824–838.

Dodt HU, Zieglgänsberger W. Visualizing unstained neurons in living brain slices by infrared DIC-videomicroscopy. Brain Res 1990;537:333–336. [PubMed: 2085783]

Erlichman JS, Hewitt A, Damon TL, Hart M, Kurascz J, Li A, Leiter JC. Inhibition of monocarboxylate transporter 2 in the retrotrapezoid nucleus in rats: a test of the astrocyte-neuron lactate-shuttle hypothesis. J. Neurosci 2008;28:4888–4896. [PubMed: 18463242]

Gandhi GK, Cruz NF, Ball KK, Theus SA, Dienel GA. Selective astrocytic gap junctional trafficking of molecules involved in the glycolytic pathway: Impact on cellular brain imaging. J. Neurochem 2009;110:857–869. [PubMed: 19457076]

Giaume C, McCarthy KD. Control of gap-junctional communication in astrocytic networks. Trends Neurosci 1996;19:319–325. [PubMed: 8843600]

Gordon GR, Choi HB, Rungta RL, Ellis-Davies GC, MacVicar BA. Brain metabolism dictates the polarity of astrocyte control over arterioles. Nature 2008;456:745–749. [PubMed: 18971930]

Gross PM, Sposito NM, Pettersen SE, Panton DG, Fenstermacher JD. Topography of capillary density, glucose metabolism, and microvascular function within the rat inferior colliculus. J. Cereb. Blood Flow Metab 1987;7:154–160. [PubMed: 3558498]

Halestrap AP. The mitochondrial pyruvate carrier. Kinetics and specificity for substrates and inhibitors. Biochem J 1975;148:85–96. [PubMed: 1156402]

Halestrap AP, Denton RM. Specific inhibition of pyruvate transport in rat liver mitochondria and human erythrocytes by alpha-cyano-4-hydroxycinnamate. Biochem. J 1974;138:313–316. [PubMed: 4822737]

Halestrap AP, Denton RM. The specificity and metabolic implications of the inhibition of pyruvate transport in isolated mitochondria and intact tissue preparations by alpha-cyano-4-hydroxycinnamate and related compounds. Biochem. J 1975;148:97–106. [PubMed: 1171687]

Hertz L, Peng L, Dienel GA. Energy metabolism in astrocytes: high rate of oxidative metabolism and spatiotemporal dependence on glycolysis/glycogenolysis. J. Cereb. Blood Flow Metab 2007;27:219–249. [PubMed: 16835632]

Hrabetová S, Nicholson C. Contribution of dead-space microdomains to tortuosity of brain extracellular space. Neurochem Int 2004;45:467–477. [PubMed: 15186912]

Hyder F, Patel AB, Gjedde A, Rothman DL, Behar KL, Shulman RG. Neuronalglial glucose oxidation and glutamatergic-GABAergic function. J. Cereb. Blood Flow Metab 2006;26:865–877. [PubMed: 16407855]

Kauppinen RA, Nicholls DG. Synaptosomal bioenergetics. The role of glycolysis, pyruvate oxidation and responses to hypoglycaemia. Eur. J. Biochem 1986;158:159–165. [PubMed: 2874024]

Korf J. Is brain lactate metabolized immediately after neuronal activity through the oxidative pathway? J. Cereb. Blood Flow Metab 2006;26:1584–1586. [PubMed: 16639423]

Laptook AR, Peterson J, Porter AM. Effects of lactic acid infusions and pH on cerebral blood flow and metabolism. J. Cereb. Blood Flow Metab 1988;8:193–200. [PubMed: 3343294]

Lear J. Glycolysis: Link between PET and proton MR spectroscopic studies of the brain. Radiology 1990;174:328–330. [PubMed: 2153309]

Lear J, Ackermann RF. Why the deoxyglucose method has proven so useful in cerebral activation studies: The unappreciated prevalence of stimulation-induced glycolysis. J. Cereb. Blood Flow Metab 1989;9:911–913. [PubMed: 2584281]

Mangia S, Giove F, Tkác I, Logothetis NK, Henry PG, Olman CA, Maraviglia B, Di Salle F, Uğurbil K. Metabolic and hemodynamic events after changes in neuronal activity: current hypotheses, theoretical predictions and in vivo NMR experimental findings. J. Cereb. Blood Flow Metab 2009a; 29:441–463. [PubMed: 19002199]

Mangia S, Simpson IA, Vannucci SJ, Carruthers A. The in vivo neuron-to-astrocyte lactate shuttle in human brain: evidence from modeling of measured lactate levels during visual stimulation. J. Neurochem 2009b;109:55–62. [PubMed: 19393009]

Manning Fox JE, Meredith D, Halestrap AP. Characterization of human monocarboxylate transporter 4 substantiates its role in lactic acid efflux from skeletal muscle. J. Physiol 2000;529:285–293. [PubMed: 11101640]

McKenna MC, Tildon JT, Stevenson JH, Hopkins IB, Huang X, Couto R. Lactate transport by cortical synaptosomes from adult rat brain: characterization of kinetics and inhibitor specificity. Dev. Neurosci 1998;20:300–309. [PubMed: 9778566]

McKenna MC, Hopkins IB, Carey A. Alpha-cyano-4-hydroxycinnamate decreases both glucose and lactate metabolism in neurons and astrocytes: implications for lactate as an energy substrate for neurons. J. Neurosci. Res 2001;66:747–754. [PubMed: 11746398]

Moyer JR Jr, Brown TH. Methods for whole-cell recording from visually preselected neurons of perirhinal cortex in brain slices from young and aging rats. J. Neurosci. Methods 1998;86:35–54. [PubMed: 9894784]

Pellerin L, Magistretti PJ. Glutamate uptake into astrocytes stimulates aerobic glycolysis: A mechanism coupling neuronal activity to glucose utilization. Proc. Natl. Acad. Sci 1994;91:10625–10629. [PubMed: 7938003]

Pellerin L, Bouzier-Sore AK, Aubert A, Serre S, Merle M, Costalat R, Magistretti PJ. Activity-dependent regulation of energy metabolism by astrocytes: an update. Glia 2007;55:1251–1262. [PubMed: 17659524]

Ramírez BG, Rodrigues TB, Violante IR, Cruz F, Fonseca LL, Ballesteros P, Castro MM, García-Martín ML, Cerdán S. Kinetic properties of the redox switch/redox coupling mechanism as determined in primary cultures of cortical neurons and astrocytes from rat brain. J. Neurosci. Res 2007;85:3244–3253. [PubMed: 17600826]

Rennels ML, Gregory TF, Blaumanis OR, Fujimoto K, Grady PA. Evidence for a 'paravascular' fluid circulation in the mammalian central nervous system, provided by the rapid distribution of tracer protein throughout the brain from the subarachnoid space. Brain Res 1985;326:47–63. [PubMed: 3971148]

Rodrigues TB, López-Larrubia P, Cerdán S. Redox dependence and compartmentation of [^{13}C]pyruvate in the brain of deuterated rats bearing implanted C6 gliomas. J. Neurochem 2009;109:237–245. [PubMed: 19393033]

Rouach N, Koulakoff A, Abudara V, Willecke K, Giaume C. Astroglial metabolic networks sustain hippocampal synaptic transmission. Science 2008;322:1551–1555. [PubMed: 19056987]

Schurr A. Lactate: the ultimate cerebral oxidative energy substrate? J. Cereb. Blood Flow Metab 2006;26:142–152. [PubMed: 15973352]

Simpson IA, Carruthers A, Vannucci SJ. Supply and demand in cerebral energy metabolism: the role of nutrient transporters. J. Cereb. Blood Flow Metab 2007;27:1766–1791. [PubMed: 17579656]

Sims NR. Rapid isolation of metabolically active mitochondria from rat brain and subregions using Percoll density gradient centrifugation. J. Neurochem 1990;55:698–707. [PubMed: 2164576]

Sokoloff L, Reivich M, Kennedy C, Des Rosiers MH, Patlak CS, Pettigrew KD, Sakurada O, Shinohara M. The [^{14}C]deoxyglucose method for the measurement of local glucose utilization: theory, procedure, and normal values in the conscious and anesthetized albino rat. J. Neurochem 1977;28:897–916. [PubMed: 864466]

Stout RF Jr. Spray DC, Parpura V. Astrocytic 'power-grid': Delivery upon neuronal demand. Cell Science Reviews 2009;5:34–43.

Tabernero A, Giaume C, Medina JM. Endothelin-1 regulates glucose utilization in cultured astrocytes by controlling intercellular communication through gap junctions. Glia 1996;16:187–195. [PubMed: 8833189]

Tabernero A, Medina JM, Giaume C. Glucose metabolism and proliferation in glia: role of astrocytic gap junctions. J. Neurochem 2006;99:1049–1061. [PubMed: 16899068]

van Hall G, Strømstad M, Rasmussen P, Jans O, Zaar M, Gam C, Quistorff B, Secher NH, Nielsen HB. Blood lactate is an important energy source for the human brain. J. Cereb. Blood Flow Metab 2009;29:1121–1129. [PubMed: 19337275]

Vannucci SJ, Simpson IA. Developmental switch in brain nutrient transporter expression in the rat. Am. J. Physiol. Endocrinol. Metab 2003;285:E1127–E1134. [PubMed: 14534079]

Yamanishi S, Katsumura K, Kobayashi T, Puro DG. Extracellular lactate as a dynamic vasoactive signal in the rat retinal microvasculature. Am. J. Physiol. Heart Circ. Physiol 2006;290:H925–H934. [PubMed: 16299264]

Zhou M, Diwu Z, Panchuk-Voloshina N, Haugland RP. A stable nonfluorescent derivative of resorufin for the fluorometric determination of trace hydrogen peroxide: applications in detecting the activity of phagocyte NADPH oxidase and other oxidases. Anal. Biochem 1997;253:162–168. [PubMed: 9367498]

Zielke HR, Zielke CL, Baab PJ. Direct measurement of oxidative metabolism in the living brain by microdialysis: a review. J. Neurochem 2009;109:24–29. [PubMed: 19393005]

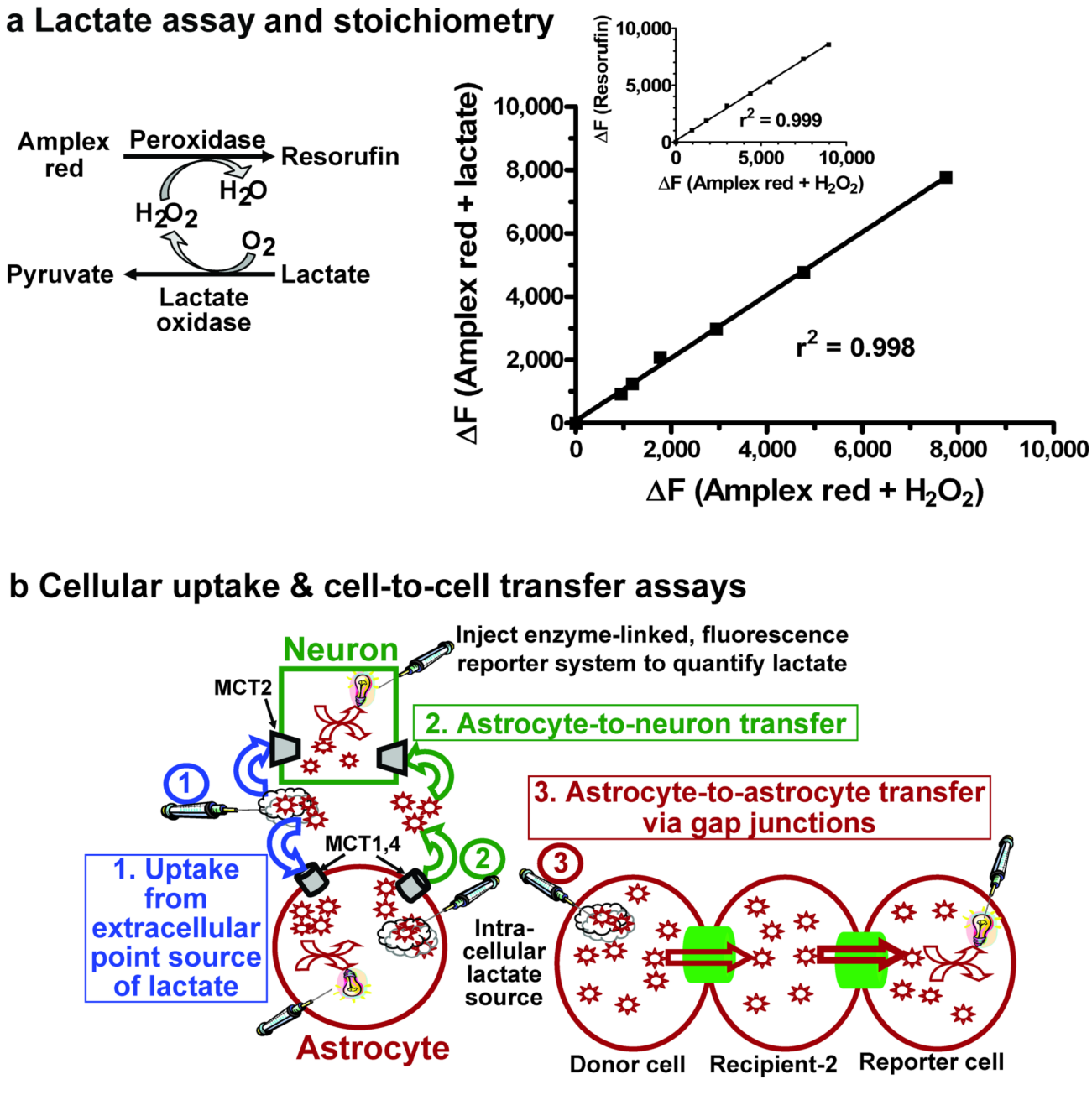

Figure 1. Lactate oxidase system to assay lactate trafficking among astrocytes and neurons

(a) Left panel: Two enzymes, lactate oxidase and horseradish peroxidase, are used to oxidize lactate and generate resorufin, a fluorescent molecule. Right panel: The stoichiometry of the reaction carried out by horseradish peroxidase (Amplex red plus hydrogen peroxide) and the coupled reaction (Amplex red plus lactate) is 1:1. The inset shows the 1:1 relationship between fluorescence of known quantities of resorufin and oxidation of known amounts of H_2O_2. Plotted values are representative of 6 independent assays. (b) Schematic of three types of lactate transfer assays: lactate uptake from a point source in extracellular fluid into neurons and astrocytes (scheme 1, blue arrows), lactate shuttling from astrocytes to neurons (scheme 2,

green arrows), and lactate trafficking among gap junction-coupled astrocytes (scheme 3, red arrows).

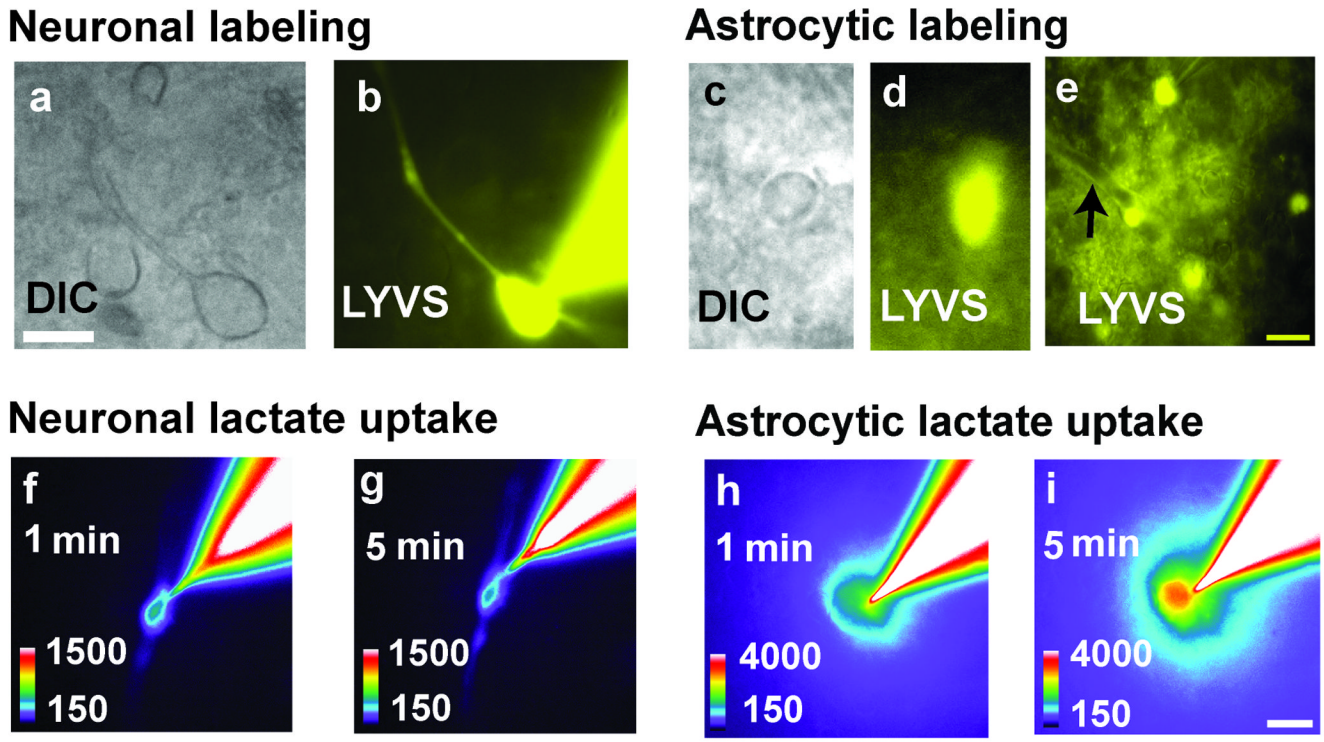

Figure 2. Single cell responses to uptake extracellular lactate

Neurons (a) or astrocytes (c) were identified under differential interference contrast (DIC) in slices of inferior colliculus from adult rat brain, and a single cell was impaled with a micropipette containing the enzymatic reaction mixture plus a gap junction-permeable fluorescent dye, Lucifer yellow VS (LYVS). Dye spread labeled the impaled neuron (b) and astrocyte (d), plus gap junction-coupled astrocytes (e) and their perivascular structures (arrow), i.e., astrocytic endfeet. Then a second micropipette containing L-lactate was placed in extracellular fluid about 2 μm from the membrane of the cell containing the enzymatic reporter system (Fig 1b, scheme 1). Lactate uptake into neurons (f, g) and astrocytes (h, i) generated a fluorescent response that increased with time, more in astrocytes (i) than neurons (g). Scale bars = 10 μm and apply to all panels.

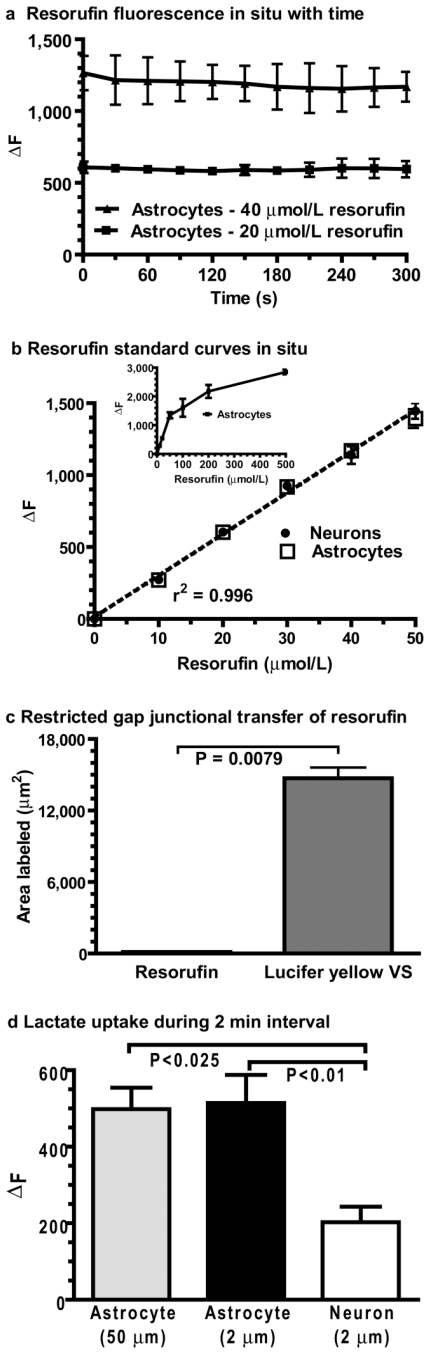

Figure 3. Standardization of the lactate assay in neurons and astrocytes in slices of inferior colliculus from adult rat brain

(a) Impaling a single cell with a micropipette containing known concentrations of resorufin gives a stable fluorescence response with repeated sampling with 100 ms exposures at 30 s intervals (n=3/group). (b) The linear ranges of standard curves were identified by diffusing known concentrations of resorufin into single neurons and astrocytes (n = 5/data point); the equation of the linear regression line is y = 28.8x + 14.1. The inset shows the non-linear fluorescence response of higher resorufin concentrations. (c) Area labeled by co-diffusion of Lucifer yellow plus resorufin into single astrocytes (n = 5/group; paired t test). (d) Net increase in fluorescence (ΔF) due to lactate uptake from extracellular fluid into astrocytes and neurons

located at the indicated distances from the tip of the micropipette containing L-lactate (10 mmol/L). P values for indicated comparisons were determined by ANOVA and Tukey's test (n=5 for astrocytes and neurons at 2 μm, n=4 for astrocytes at 50 μm). Values are means and vertical bars represent ±1SD; if not visible, SDs are smaller than the symbol.

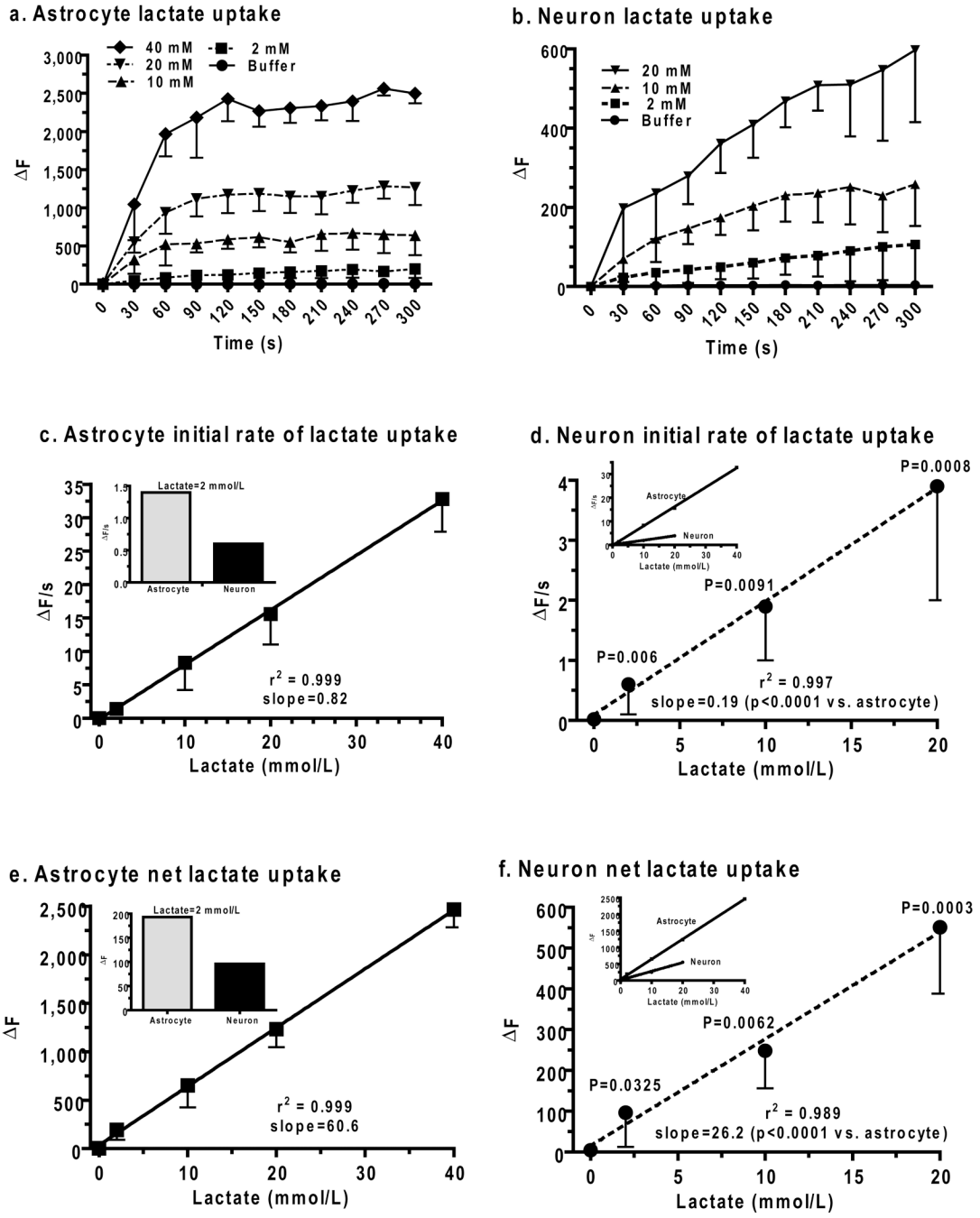

Figure 4. Lactate uptake into astrocytes and neurons from extracellular space

Time courses of lactate uptake (ΔF) from a micropipette placed about 2 μm from the membrane of astrocytes (a) and neurons (b) in slices of adult rat inferior colliculus (see Fig. 1b, Scheme 1, blue arrows). Initial lactate uptake rates (ΔF/s, c, d) were calculated as the slope during the first 60 s (a, b), and net lactate uptake (ΔF, e, f) was calculated as the mean of the values measured at 240–300 s (a, b). Values at zero lactate (a–f) are endogenous responses to impaling the reporter cell and placing a buffer-containing pipette outside the cell; similar values were obtained by only placing the reporter pipette into the cell (data not shown; n= 5/group for astrocytes and neurons). Values are means and vertical bars are 1 SD. For astrocytes: n = 5, 15, 8, 5, and 5 for buffer, 2,10, 20, and 40 mmol/L lactate, respectively. For neurons: n = 5,

10, 5, and 5 for buffer, 2,10, and 20 mmol/L lactate, respectively. P values for comparisons (unpaired, two-tailed t test) between corresponding values for astrocytes and neurons at each lactate concentration are shown on the neuron graphs. The goodness of fit (r^2) and slope (all slopes were different from zero, $P < 0.006$) are indicated for the linear regression lines for astrocytic (solid lines) and neuronal (dashed lines) lactate initial uptake rates (c, d) and net lactate uptake (e, f). Significant differences in the respective slopes of the astrocytic and neuronal regression lines were identified with the unpaired, two-tailed t test and are indicated in neuron graphs (d, f).

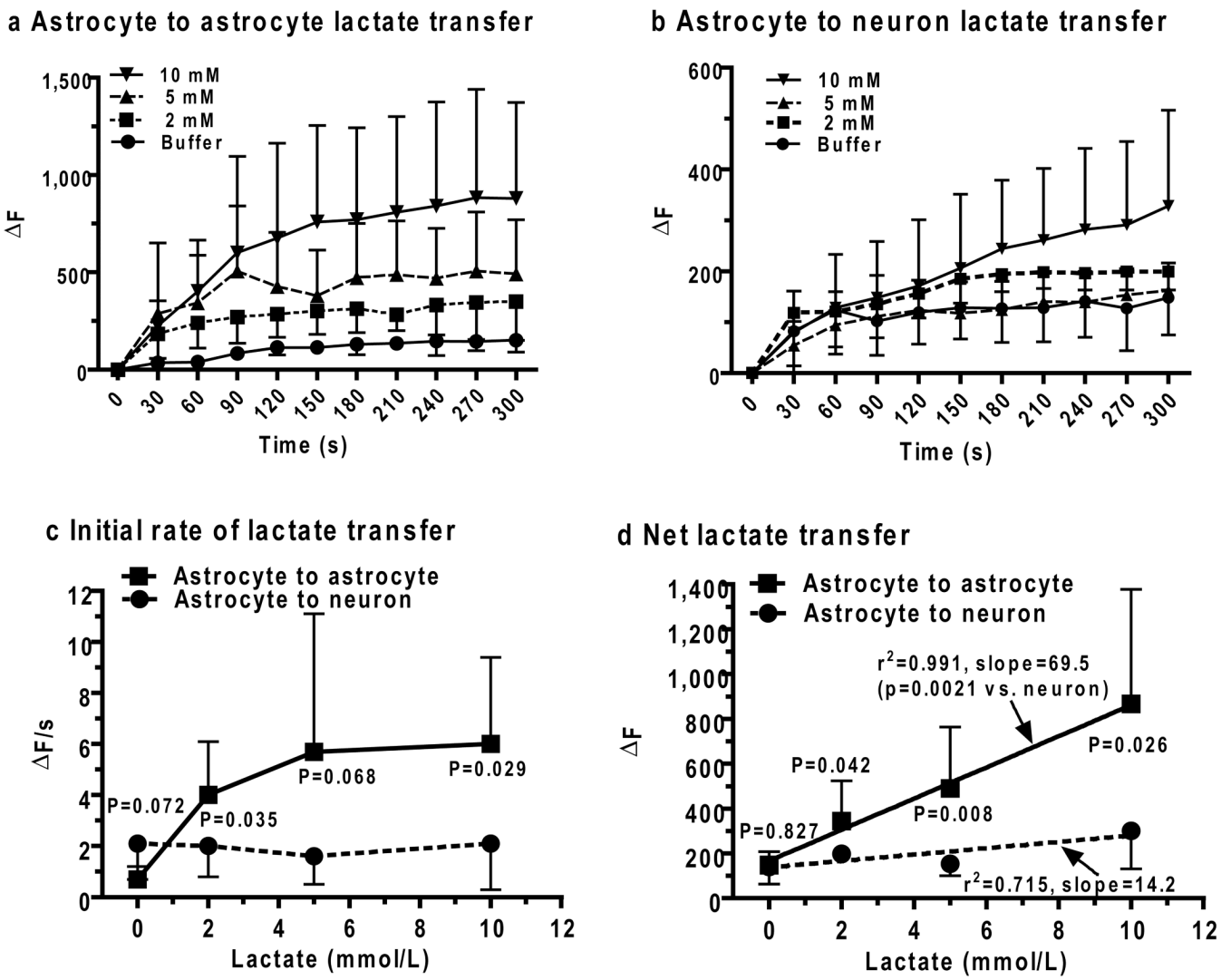

Figure 5. Lactate trafficking among gap junction-coupled astrocytes and from astrocytes to neurons

Concentration-dependent temporal profiles of lactate shuttling from (a) one astrocyte to another astrocyte (Fig. 1b, Scheme 3, red arrows) or (b) an astrocyte to a neuron (Fig. 1b, Scheme 2, green arrows) in slices of adult rat inferior colliculus were assayed by inserting a lactate-containing pipette into an astrocyte located 50 ± 5 μm from the enzyme-containing reporter cell. Initial lactate uptake rates (c, ΔF/s) and net lactate uptake (d, ΔF) were calculated from the 0–60 and 240–300 s intervals of the time courses. Lines connect the points in panels a–c. P values (unpaired, two-tailed t test) are indicated for comparisons between neuronsv and astrocytes at each lactate concentration and for the slopes of the linear regression lines in panel d for astrocytic (solid lines) and neuronal (dashed lines) net lactate uptake. Zero lactate denotes the endogenous response to impaling the reporter cell and placing a pipette outside the cell; similar control values were obtained by only placing the reporter pipette into the cell, with no second pipette (not shown, n= 5/group for astrocytes and neurons).Values are means; vertical bars are 1SD. For astrocytes: n = 5, 8, 7, and 7, for buffer, 2, 5, and 10, lactate, respectively. For neurons: n = 5, 8, 7, and 6 for buffer, 2, 5, and 10, lactate, respectively. Astrocyte-to-astrocyte lactate (10 mmol/L) transfer was gap junction-dependent; ΔF = 866 ± 511 (n = 7)

and 230 ± 140 (n=5), in the absence and presence of octanol (gap junction inhibitor), respectively.

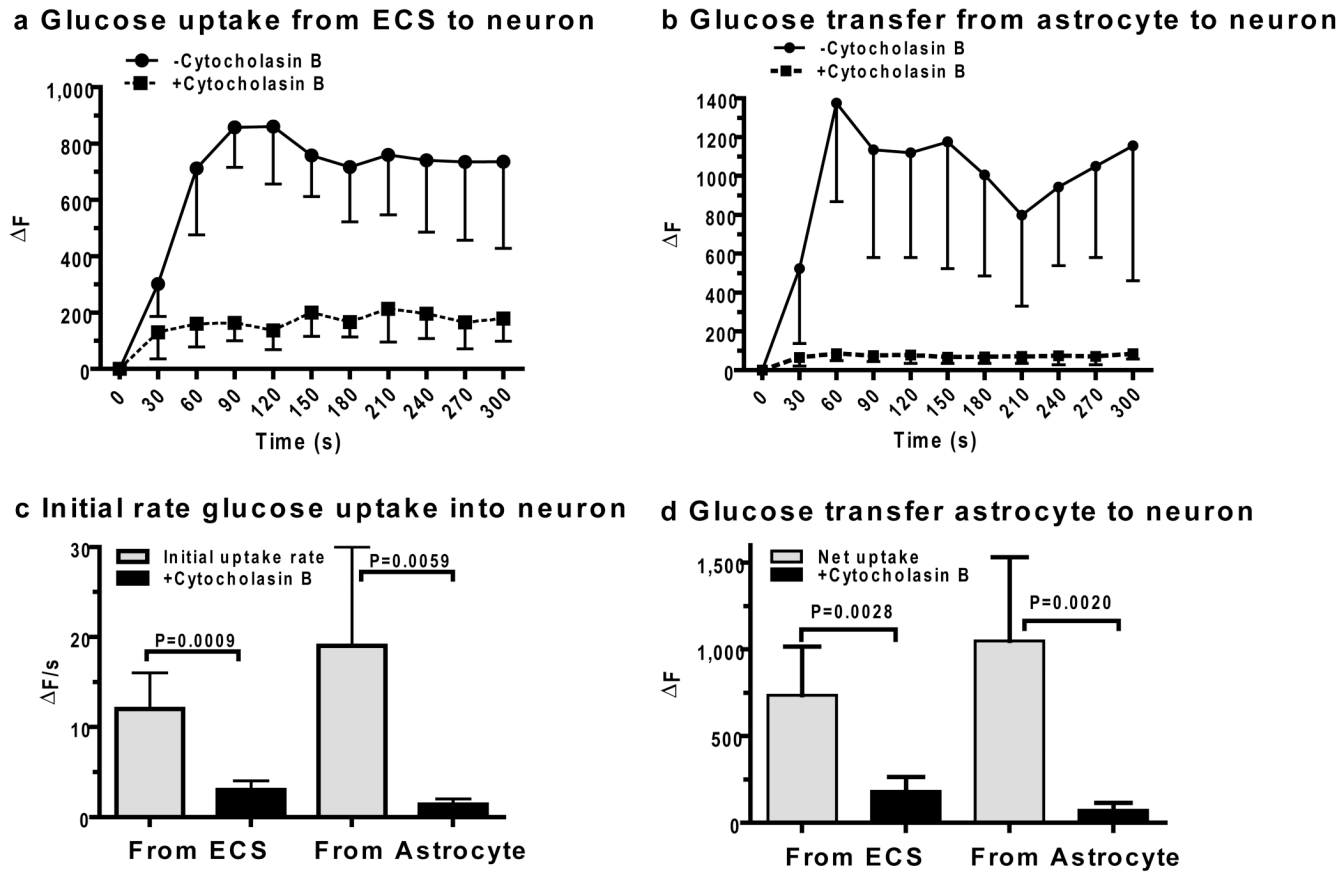

Figure 6. Glucose delivery to neurons from astrocytes

Neuronal glucose uptake from a micropipette containing 20 mmol glucose/L and located 2 μm from the neuronal membrane (a) or from an astrocyte impaled with a micropipette containing 20 mmol glucose/L and located 30–50 μm from the neuron (b) in slices of adult rat inferior colliculus. Coupled glucose oxidase-horseradish peroxidase assays were carried out in the absence or presence of cytochalasin B (10 μmol/L in the perfusion fluid) to block glucose transporters. Initial glucose uptake rates (c) and net transfer (d) were calculated from values over the 0–60s and 240–300s intervals (a, b). P values for indicated comparisons were determined with the unpaired, two-tailed t test (n=5/group).

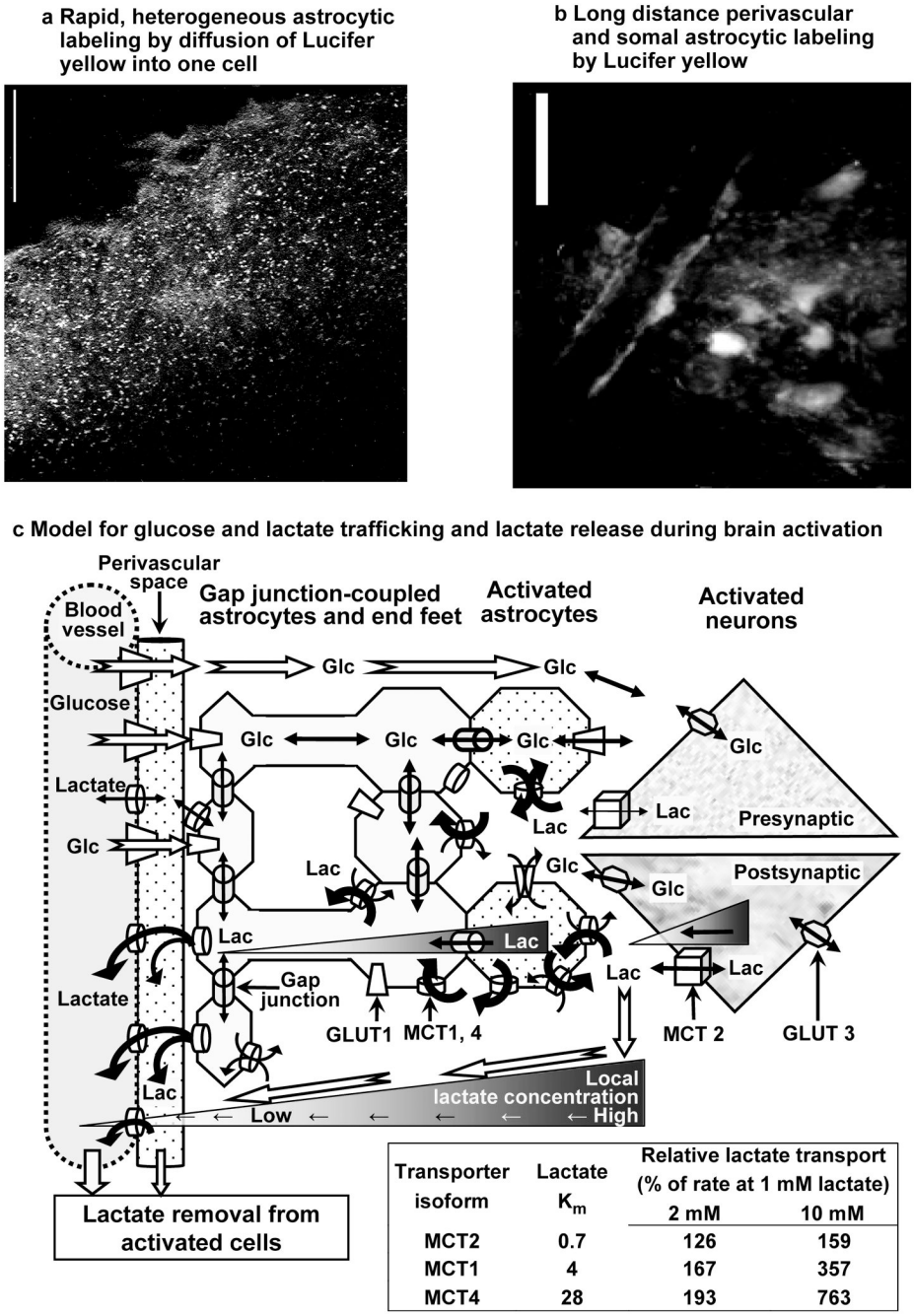

Figure 7. Dye and metabolite trafficking via gap junction-coupled astrocytes

Astrocytes in the adult rat inferior colliculus are highly coupled by gap junctions, and diffusion of Lucifer yellow VS into a single astrocyte for 5 min labels thousands of cells (a, scale bar = 100 μm) and their perivascular endfeet (b, scale bar = 25 μm). (c) A model emphasizing diffusion and transporter-mediated pathways for (i) uptake of glucose from blood into brain and distribution within tissue and (ii) clearance of lactate from glycolytic domains via intracellular and extracellular routes *during brain activation*. For clarity, the tortuosity of extracellular space, cell-cell connections, and more distant non-activated cells are not portrayed. Glucose and lactate fluxes in interstitial fluid and within cells follow their local concentration gradients; hypothetical lactate gradients during brain activation are illustrated

as gray-scales in intracellular and extracellular fluid and from brain to blood and thicker lines through transporters. In normal activated brain lactate is generated intracellularly and will be dispersed by diffusion and carrier-mediated co-transport with H^+, which is influenced by local pH. Because Caesar et al. (2008) reported that metabolic responses (increased blood flow, $CMRO_2$, CMR_{glc}, extracellular lactate level) to stimulation in the cerebellum were blocked by postsynaptic AMPA receptor blockers, lactate gradients in postsynaptic neuronal domains are emphasized; recent modeling studies (Simpson et al., 2007; Mangia et al., 2009b) also support predominant neuronal glucose utilization and neuronal lactate generation, but astrocytic glycolytic activity is also likely. Because astrocytes have a faster and greater capacity for uptake and lactate trafficking than neurons (Fig. 4, Fig. 5), lactate dispersal among thousands of astrocytes via gap junctions (a) and to distant perivascular fluid (b) is likely to facilitate rapid lactate release from activated tissue domains by diffusion and transport among cells, ultimately to blood (c). Lactate in interstitial fluid is also expected to diffuse down its extracellular concentration gradient to perivascular space and blood (c) Relative rates of lactate transport (table in c) were calculated for each monocarboxylic acid transporter (MCT) isoform, assuming Michaelis-Menten kinetics and using K_m values from Table 1 of Manning Fox et al. (2000). MCT2 is located mainly in neurons whereas MCT1 and MCT4 are mainly in astrocytes (Bergersen, 2007). Abbreviations: Glc, glucose; Lac, lactate; MCT, monocarboxylic acid transporter; GLUT, glucose transporter.